Arabian Journal of Chemistry (2015) xxx, xxx–xxx

King Saud University

Arabian Journal of Chemistry

www.ksu.edu.sa
www.sciencedirect.com

ORIGINAL ARTICLE

Studies on green synthesized silver nanoparticles using *Abelmoschus esculentus* (L.) pulp extract having anticancer (*in vitro*) and antimicrobial applications

Md. Masud Rahaman Mollick [a], Dipak Rana [b], Sandeep Kumar Dash [c], Sourav Chattopadhyay [c], Biplab Bhowmick [a], Dipanwita Maity [a], Dibyendu Mondal [a], Sutanuka Pattanayak [d], Somenath Roy [c], Mukut Chakraborty [d,*], Dipankar Chattopadhyay [a,*]

[a] *Department of Polymer Science and Technology, University of Calcutta, 92 A. P. C. Road, Kolkata 700 009, India*
[b] *Department of Chemical and Biological Engineering, Industrial Membrane Research Institute, University of Ottawa, 161 Louis Pasteur St., Ottawa, ON K1N 6N5, Canada*
[c] *Department of Human Physiology with Community Health, Immunology and Microbiology Laboratory, Vidyasagar University, Midnapore 721 102, India*
[d] *Department of Chemistry, West Bengal State University, Barasat, Kolkata 700 126, India*

Received 21 January 2015; accepted 26 April 2015

KEYWORDS

Silver nanoparticles;
Abelmoschus esculentus (L);
Anticancer activity (*in vitro*);
Nitric oxide release;
Caspase-3 activity;
Antimicrobial activity

Abstract Silver nanoparticles (Ag NPs) were successfully synthesized using $AgNO_3$ via an eco-friendly and simple green route using *Abelmoschus esculentus* (L.) pulp extract at room temperature. The phytochemicals present in *A. esculentus* (L.) pulp extract were used both as a reducing and a stabilizing agent for the synthesis of Ag NPs. The stabilization of Ag NPs with phytochemicals was justified using Fourier-transform infrared spectroscopy. The size of the as-synthesized Ag NPs was examined using dynamic light scattering and confirmed by transmission electron microscopy. The crystalline nature of Ag NPs had been identified using X-ray diffraction. The present study demonstrated the efficacy of Ag NPs against Jurkat cells *in vitro*. Our study also showed that the IC_{50} dose of Ag NPs leads to the increase in intracellular reactive oxygen species and

* Corresponding authors. Tel.: +91 33 2350 1397/6996/6387/8386; fax: +91 33 2351 9755.
E-mail address: dipankar.chattopadhyay@gmail.com (D. Chattopadhyay).

Peer review under responsibility of King Saud University.

Production and hosting by Elsevier

http://dx.doi.org/10.1016/j.arabjc.2015.04.033

Please cite this article in press as: Mollick, M.M.R. et al., Studies on green synthesized silver nanoparticles using *Abelmoschus esculentus* (L.) pulp extract having anticancer (*in vitro*) and antimicrobial applications. Arabian Journal of Chemistry (2015), http://dx.doi.org/10.1016/j.arabjc.2015.04.033

significantly diminished mitochondrial membrane potential, indicating the effective involvement of apoptosis in cell death. The synthesized Ag NPs also exhibited good antimicrobial activity against different gram class bacteria.

1. Introduction

Effective application of material science requires the tuning of the material morphology as it plays an essential role in controlling the basic properties of the materials. To achieve the same, the fabrication of nano-materials of definite composition, precise shape and particular size is a promising area of research in the field of nanotechnology. In comparison to bulk materials, nanoparticles (NPs) provide a range of exclusive chemical, optical, mechanical, electronic and magnetic properties (Bhushan, 2004), due to three main reasons, (i) the size of NPs is comparable to the Bohr radius of the excitons, (ii) the surface atoms constitute a considerable fraction of the total number of the atoms of the NPs and (iii) the natural size of the NPs is comparable with the size of the molecules. Since ancient times, silver has long been recognized as an effective antimicrobial agent for the treatment of diseases, food preservation, and purification of water (Silver, 2003). A number of techniques are available for the synthesis of silver NPs (Ag NPs), such as chemical (Maity et al., 2011; Sun et al., 2002), electrochemical (Yin et al., 2003), radiation (Dimitrijevic et al., 2001), photochemical methods (Callegari et al., 2003), Langmuir–Blodgett (Swami et al., 2004; Zhang et al., 2006), and biological techniques (Naik et al., 2002). However, the majority of these being energy and capital intensive processes deal with various toxic chemicals and non-polar solvents that hinder the efficacy of these NPs toward biomedical applications. The biogenic synthesis of metal NPs reduces these hazards through the elimination/minimization of generated waste and the implementation of sustainable processes. Biological methods of NPs synthesis using microorganisms (Klaus et al., 1999; Konishi et al., 2007), enzymes (Willner et al., 2006), and plant or plant extracts (Shankar et al., 2004) have been studied as possible eco-friendly alternatives to chemical and physical methods.

Jose Yacaman and co-workers first reported the formation of gold and silver NPs using living plants (Gardea-Torresdey et al., 2002, 2003). Song and Kim (2009) prepared Ag NPs using five different leaf extracts (Pine, Persimmon, Ginkgo, Magnolia, and Platanus) and compared the extracellular synthesis of Ag NPs. They showed that among the five, magnolia leaf broth had the best reducing property in terms of synthesis rate and conversion to Ag NPs. Reaction kinetics showed that only 11 min was required for more than 90% conversion at the reaction temperature of 95 °C using magnolia leaf broth. A simple technique using Sugar apple (*Annona squamosa*) peel extract was used by Kumar et al. (2012) and Roopan et al. (2015) to synthesize Ag NPs and SnO_2 NPs. They have demonstrated the effect of temperature on the Ag NPs synthesis and also proposed a plausible mechanism for its reduction. The synthesized SnO_2 NPs exhibited good efficiency on hepatocellular carcinoma cell line. Mollick et al. (2012) reported synthesis of Ag NPs through a reliable, eco-friendly and green route using *Paederia foetida L.* leaf extract as a reducing cum stabilizing agent. Shankar et al. (2004) carried out the synthesis of pure metallic NPs of silver and gold by the reduction of Ag^+ and Au^{3+} ions using Neem (*Azadirachta indica*) leaf broth. Sastry and co-workers (Mukherjee et al., 2001a, 2001b) synthesized metal NPs using eukaryotic organisms such as *Verticillium* sp. They suggested that the processing and handling of the biomass was simpler in the case of fungi in comparison with the bacteria. In another work, Ag NPs have been derived using green kondagogu gum as a template (Kora et al., 2010). Roopan and co-workers (Roopan et al., 2013; Roopan and Elango, 2015) have used extracts from different parts of *Cocos nucifera* to synthesize Ag NPs and Au NPs under different physical, chemical and biological conditions. It has also been reported that acacia gum (Mohan et al., 2007) can be utilized both as a reducing as well as stabilizing agent for the Ag NPs biosynthesis. To date, several approaches have been carried out for the biogenic synthesis of Ag NPs using various natural products such as latex from *Alfalfa sprouts* (Gardea-Torresdey et al., 2003), *Jatropha curcas* (Bar et al., 2009a), geranium leaves plant extract (Shankar et al., 2003), and the stem derived callus extract of bitter apple (*Citrullus colocynthis*) (Satyavani et al., 2011). Green synthesis of Ag NPs was carried out by Kumar et al. (2014) using *Alternanthera dentata* leaf extract and the synthesized NPs showed good antimicrobial activity. Recently, Madhumitha et al. (2015) have nicely assimilated the different methods of synthesis of Ag NPs and their antimicrobial studies.

Among all the noble metals, silver has attracted major attention due to its disinfecting nature and tremendous medicinal value to culinary items as well as showing enormous effectiveness as an anticancer agent. Moreover, several salts of silver and their derivatives are commercially manufactured as antimicrobial agents (Hernandez-Sierra et al., 2008; Krutyakov et al., 2008). In small concentrations, silver is safe for human cells, but lethal for bacteria and viruses (Saha et al., 2010; Sarkar et al., 2011; Sharma et al., 2009). The antibacterial property of Ag NPs has been studied by a number of researchers (Bankura et al., 2012; Maity et al., 2012). Recently, Mishra et al. (2011) tested the antibacterial action of Ag NPs against different pathogenic bacteria. Worldwide study shows that cancer is one of the leading causes of death worldwide after cardiovascular diseases (Garrett and Workman, 1999). Leukemia is a major type of cancer affecting a significant part of the population, especially children. In fact, leukemia is the most frequent childhood cancer, with 26% of all cases, and 30% mortality (Canadian Cancer Society, 2005). Considering the various limitations as well as severe side effects of current anti-cancer drugs, there is an emerging need to develop new classes of therapeutic agents comparatively

Please cite this article in press as: Mollick, M.M.R. et al., Studies on green synthesized silver nanoparticles using *Abelmoschus esculentus* (L.) pulp extract having anticancer (*in vitro*) and antimicrobial applications. Arabian Journal of Chemistry (2015), http://dx.doi.org/10.1016/j.arabjc.2015.04.033

with better bio compatibility as well as efficacy. Modern research regarding the development of metal-based anticancer drugs began with the discovery of the platinum (II) complex cis-platin by Barnett Rosenberg in the 1960s (Rosenberg et al., 1969). Recent advancements in nanotechnology spread the area of research based on meal based NPs having biomedical applications. Ag NPs, in particular, have been the focus of increasing interest due to their excellent contribution for therapeutic purposes. In recent years, green synthesis of NPs has been an easy, efficient and eco-friendly approach for NPs preparation (Devi et al., 2012). Earlier studies show that the cytotoxicity of synthesized Ag NPs is related to the involvement of the level of cellular reactive oxygen species (ROS) and mitochondrial membrane disruption (AshaRani et al., 2009; Sanpui et al., 2011). However, there is a lack of detailed study regarding the anticancer effects of green synthesized Ag NPs. To the best of our knowledge, no study has been undertaken to demonstrate the *in vitro* anti-proliferative effects of green synthesized Ag NPs against the human T-cell lymphoma (Jurkat).

In this article, we have reported a simple one-step green approach to synthesizing extracellular Ag NPs using *Abelmoschus esculentus* (L.) pulp extract. The ingredients present in the *A. esculentus* (L.) pulp extract are used as an effective reducing, as well as stabilizing agent. *A. esculentus* (L.) pulp, being a purely natural product with medicinal value, has drawn our interest toward the green synthesis of Ag NPs via an eco-friendly process. The present study also tried to validate the possible *in vitro* anti-proliferative effects of green synthesized Ag NPs against the Jurkat cell line. The synthesized Ag NPs are an efficient tool showing sufficient resistance against different gram class bacteria.

2. Experimental

2.1. Materials

Analytical grade silver nitrate ($AgNO_3$) was purchased from Merck Mumbai, India, and used as received without further purification. The *A. esculentus* (L.) was collected from the local market of our institute.

2.2. Culture media and chemicals

RPMI (Roswell Park Memorial Institute) medium 1640, N-acetyl-L-cysteine (NAC, $\geqslant$99%), N-(1 naphthyl)-1,2-ethylenediamine dihydrochloride ($>$98%), sulfanilamide ($\geqslant$99%), penicillin, and streptomycin were procured from Sigma, St. Louis, MO. 4′,6-Diamidino-2-phenylindole dihydrochloride (DAPI) was purchased from Sigma-Aldrich. Fetal bovine serum (FBS) was purchased from GIBCO/Invitrogen. Commercially available dimethyl sulfoxide (DMSO), sodium dodecyl sulfate (SDS), Rhodamin 123, and 3-(4,5-dimethyl-2-thiazolyl)-2,5-diphenyl-tetrazolium bromide (MTT) reagent were purchased from HiMedia Laboratories Pvt. Ltd., Mumbai, India. All other chemicals were from Merck Ltd. and SRL Pvt. Ltd. Mumbai (India) and were of the highest purity grade available. Solvents were dried according to the standard procedure and distilled prior to use (Perrin et al., 1980).

2.3. Synthesis of silver nanoparticles

A fixed amount of small slices of fresh *A. esculentus* (L.) pulp was put into triple distilled water and left for 2 h in order to maximize the diffusion of the materials present in the *A. esculentus* (L.) pulp into triple distilled water. After that, the pulps were taken out from the medium and the solution was subjected to centrifugation to remove any solid impurities present in the stock. The supernatant was carefully collected and used as the *A. esculentus* (L.) pulp extract. The extract was mixed with the aqueous solution of 1 mM silver nitrate (4:1 v:v) at room temperature with continuous stirring for approximately 9 h. Then, the colloidal solution was left undisturbed for 27 h at room temperature. The formation of Ag NPs was confirmed by observing the color change of this colloid solution from colorless to light yellow.

2.4. Cell lines culture and maintenance

Jurkat cell line (Human T-cell lymphoma) was obtained from the National Centre for Cell Science (NCCS), Pune, India. This cell line was cultivated and maintained in RPMI medium 1640 complete media supplemented with 10% heat-inactivated fetal bovine serum (FBS), 100 U/ml penicillin, 100 μg/ml streptomycin and 4 mM L-glutamine under 5% CO_2 and a 95% humidified atmosphere at 37 °C in a CO_2 incubator. Cells were used for different experiments until the number of cells reaches at 1.0×10^6 cells/ml.

2.5. Drug preparation

One milligram per milliliter stock of Ag NPs was prepared by concentrating the prepared Ag NPs containing solution using a rotary evaporator. It was then serially diluted with RPMI media to prepare working concentrations.

2.6. Experimental design

The Jurkat cells were divided into 11 groups. Each group contained 6 petri dishes (2×10^4 cells in each). The following groups were considered for the experiment and cultured for 24 h:

Group I: Control i.e., Cells + culture media, **Group II:** Cells + 1 μg/ml Ag NPs in culture media, **Group III:** Cells + 5 μg/ml Ag NPs in culture media, **Group IV:** Cells + 10 μg/ml Ag NPs in culture media, **Group V:** Cells + 25 μg/ml Ag NPs in culture media, and **Group VI:** Cells + 50 μg/ml Ag NPs in culture media.

After the treatment schedule, the cells were collected from the petri dishes separately and centrifuged at 2,200 rpm for 10 min at 4 °C to separate cells and supernatant (Dash et al., 2013). Cells were washed twice with 50 mM PBS at pH 7.4. Intact cells were used for mitochondrial membrane potential and ROS measurement.

2.7. In vitro cell viability assay (MTT assay)

The Jurkat cells were maintained in RPMI-1640 supplemented with 10% FBS, penicillin (100 U/ml), and streptomycin

Please cite this article in press as: Mollick, M.M.R. et al., Studies on green synthesized silver nanoparticles using *Abelmoschus esculentus* (L.) pulp extract having anticancer (*in vitro*) and antimicrobial applications. Arabian Journal of Chemistry (2015), http://dx.doi.org/10.1016/j.arabjc.2015.04.033

(100 μg/ml) in a humidified atmosphere of 5% CO_2 at 37 °C. The cytotoxicity of synthesized Ag NPs on Jurkat cells was determined by the MTT assay (Dash et al., 2013). Cells (2×10^4/well) were plated in 100 μl of medium/well in 96-well plates. After 48 h incubation, the cell reached confluence. Then, the cells were incubated in the presence of various concentrations of NPs suspended in RPMI medium for 24 h at 37 °C. After the treatment period, cells were centrifuged to remove the supernatant and subsequently washed with phosphate buffered saline (PBS). Then the cell were stained with 3-(4,5-dimethyl-2-thiazolyl)-2,5-diphenyl-tetrazolium bromide (MTT) at 20 μl/well (5 mg/ml) in each well of 96 well plates. After 4 h incubation, 0.04 M HCl/isopropanol was added to each well. Viable cells were determined by absorbance at 570 nm with reference at 655 nm. Measurements were performed 3 times. The absorbance at 570 nm was measured with a UV–Vis spectrophotometer using wells without sample containing cells as blanks. All experiments were performed in triplicate. The effect of the Ag NPs on the proliferation of Jurkat cells was expressed as the % cell viability using the following formula:

$$\% \text{ Proliferation} = \left[OD_{sample} - OD_{control}\right] \times 100/OD_{control}$$

2.8. Assay for antimicrobial activity of silver nanoparticles against microorganisms

Silver nanoparticles in sterilized deionized water were tested for their antibacterial activity by the agar diffusion method. Five bacterial strains, *Bacillus subtilis* [MTCC 736], *Bacillus cereus* [MTCC 306], *Pseudomonas aeruginosa* [MTCC 8158], *Micrococcus luteus* [MTCC 1538] and *Escherichia coli* [MTCC 68] were used for this analysis. These bacteria were grown in liquid nutrient agar media (HiMedia Laboratories Pvt. Ltd., Mumbai, India) for 24 h prior to the experiment and were seeded in agar plates by the pour plate technique. A cup was made using a cork borer (10 mm diameter) and was filled with the Ag NPs (0.2 mg/ml) solution and then incubated at 37 °C for 24 h. Simultaneously, the control sets (only plant extract and sterilized deionized water respectively) were also examined against the same five bacterial strains. Every experiment was repeated three times.

2.9. Characterization

2.9.1. UV–Vis absorption spectroscopy

The formation of Ag NPs was monitored by measuring the UV–Vis spectrum of the reaction medium in the wavelength range from 190 to 1100 nm. The UV–Vis absorption spectrum of the sample was performed in an Agilent 8453 Spectrophotometer, USA.

2.9.2. Dynamic light scattering (DLS)

The dynamic light scattering (also known as photon correlation spectroscopy or quasi-elastic light scattering) technique was used for determining the particle size distribution and the nature of the particle's motion in the medium. The light scattering technique of the synthesized Ag NPs was observed using a Zetasizer, Nano-ZS90 system (Malvern Inc.).

2.9.3. Transmission electron microscopy (TEM)

The morphological analysis of the resultant nanoparticles was carried out by using TEM. The sample suspension was drop casted on a carbon coated copper grid and the excess solution was removed by tissue paper and allowed to air-dry at room temperature overnight. The TEM study was monitored on a HRTEM, JEOL JEM 2010 at an accelerating voltage of 200 kV and fitted with a CCD camera.

2.9.4. X-ray diffraction (XRD)

The crystal structure of the produced Ag NPs was determined and confirmed by XRD analysis. The sample for XRD analysis was prepared by depositing the centrifuged sample on a microscopic glass slide and air-dried overnight. The diffractogram was recorded in a PANalytical, XPERT-PRO diffractrometer using Cu Kα (λ = 1.54060 Å) as an X-ray source.

2.9.5. Fourier transform infrared (FTIR) spectroscopy

For the Fourier transform infrared (FTIR) spectroscopy analysis, the vacuum dried Ag NPs were mixed with potassium bromide (KBr) and the spectra were recorded with a Perkin Elmer Spectrum Express version 1.03.00. The scanning data were obtained from the average of 47 scans in the range 4000–400 cm^{-1} with the resolution of 4 cm^{-1}.

2.9.6. For anticancer activity

2.9.6.1. Calculation of IC_{50} value. The concentration required for 50% inhibition of viability (IC_{50}) was determined graphically. Multiple linear regressions were used to compare data using the Statistica version 5.0 (Statsoft, India) software package.

2.9.6.2. Nitric oxide release assay. Jurkat cell lines (2×10^4-/well) were treated with Ag NPs at 16.15 μg/ml for 24 h. After the schedule treatment, 100 μl of Griess reagent (containing 1 part of 1% sulfanilamide in 5% phosphoric acid, and 1 part of 0.1% of N-(1 naphthyl)-1,2-ethylenediamine dihydrochloride) was added to 100 μl of supernatant, incubated at room temperature for 10 min. Readings were taken in a UV spectrophotometer at 550 nm and compared with a sodium nitrite standard curve (values ranging between 0.5 and 25 μM). The levels of nitric oxide (NO) were expressed as μM mg^{-1} protein (Mahapatra et al., 2009). All measurements were done in triplicate.

2.9.6.3. Intracellular ROS. The reactive oxygen species (ROS) measurement was performed using 2′,7′-dichlorodihydrofluor escein diacetate (H_2DCF–DA) according to the method of Roy et al. (2008). In brief, Jurkat cell lines (2×10^4/well) were treated with Ag NPs at 16.15 μg/ml for 24 h. After the schedule treatment, cells were washed with a culture media followed by incubation with 1 μg/ml H_2DCF–DA for 30 min at 37 °C. Then, the cells were washed three times with fresh culture media. DCF fluorescence was determined at 485 nm excitation and 520 nm emission using a Hitachi F-7000 Fluorescence Spectrophotometer. The cells were also observed by fluorescence microscopy (NIKON ECLIPSE LV100POL). All measurements were done in triplicate.

2.9.6.4. Measurement of mitochondrial membrane potential ($\Delta\Psi m$). The alteration of the mitochondrial membrane

potential by the spectro-fluorometric method was done according to our previous reported method (Dash et al., 2013). In brief, Jurkat cell lines (2×10^4/well) were treated with Ag NPs at 16.15 μg/ml for 24 h. After the schedule treatment, cells were washed with culture media followed by incubation with 1.5 μM Rhodamin (Rh) 123 for 10 min at 37 °C in a humidified incubator. Then, the cells were washed three times with culture media. The cellular fluorescence intensity of Rh 123 was monitored for 2 min using a Hitachi F-7000 Fluorescence Spectrophotometer. Cellular mitochondrial membrane potential was expressed as a percentage of control cells at an excitation wavelength of 493 nm and an emission wavelength of 522 nm. Both excitation and emission slit width were set to 5.0.

2.9.6.5. Cell survival after pre-treatment with ROS scavenger. To determine the role of ROS production in Ag NPs-induced cell death, Jurkat cells (2×10^4/well) were pretreated with 5 mM N-acetyl-L-cysteine (NAC) as the potent ROS scavenger, NAC (Sigma, St. Louis, MO) for 4–6 h (Hanley et al., 2009). After pre-treatment, Jurkat cells were washed two times with culture media and were exposed to Ag NPs at IC_{50} doses for 24 h. After NPs exposure, cell viability was estimated using the MTT assay (Dash et al., 2013).

2.9.6.6. Assessment of nuclear morphological changes by DAPI staining. For DAPI staining, the test cells were seeded into six well plates. A number of 2×10^4 cells/ml were treated with or without Ag NPs (0, and 16.15 μg/ml) for 24 h and were then isolated for DAPI staining according to the method of Mollick et al. (2014a). After treatment schedule, the cells were fixed with 2.5% glutaraldehyde for 15 min, permeabilized with 0.1% Triton X-100 and stained with 1 μg/ml DAPI for 5 min at 37 °C. The cells were then washed with PBS and examined by fluorescence microscopy (NIKON ECLIPSE LV100POL).

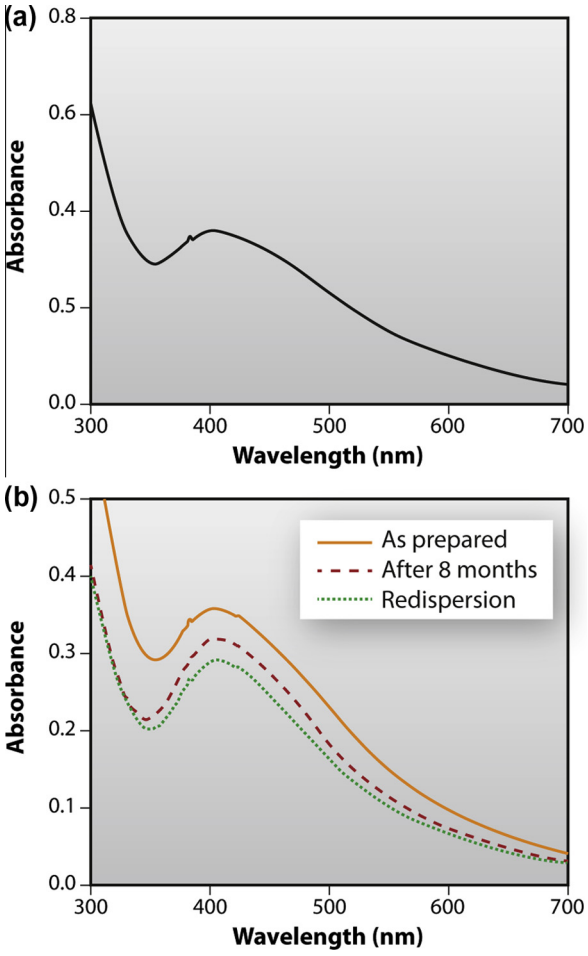

Figure 1 UV–Vis absorption spectra of (a) Ag NPs synthesized by treating 0.001 M aqueous silver nitrate solution with *Abelmoschus esculentus* (L.) pulp extract at room temperature and (b) UV–Vis absorption spectra of Ag NPs stabilized with *Abelmoschus esculentus* (L.) pulp extract (after reaction termination; after 8 months storage at room temperature; after re-dispersion of Ag NPs in the triple distilled water.

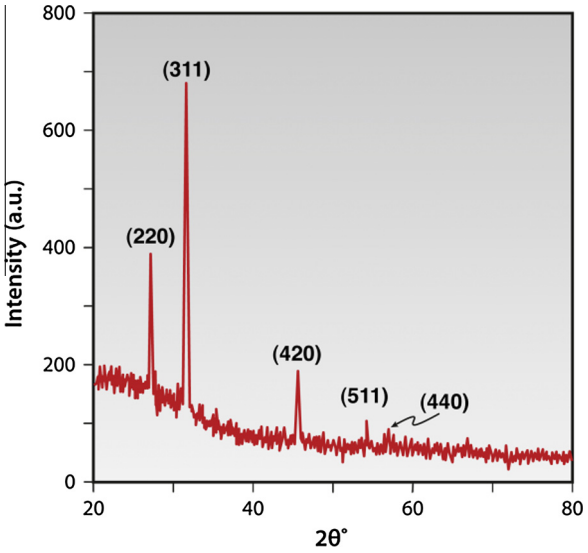

Figure 2 XRD peaks corresponding to the diffraction from (220), (311), (420), (511), and (440) planes of fcc lattice of Ag NPs.

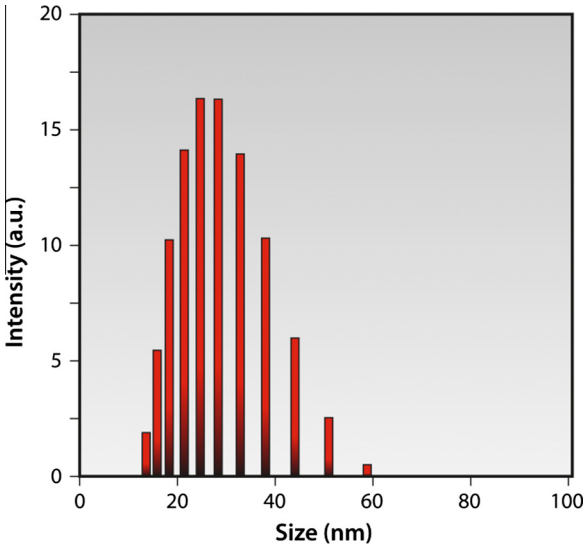

Figure 3 DLS showing particles size distribution of Ag NPs prepared by treating 0.001 M aqueous silver nitrate solution with *Abelmoschus esculentus* (L.) pulp extract at room temperature.

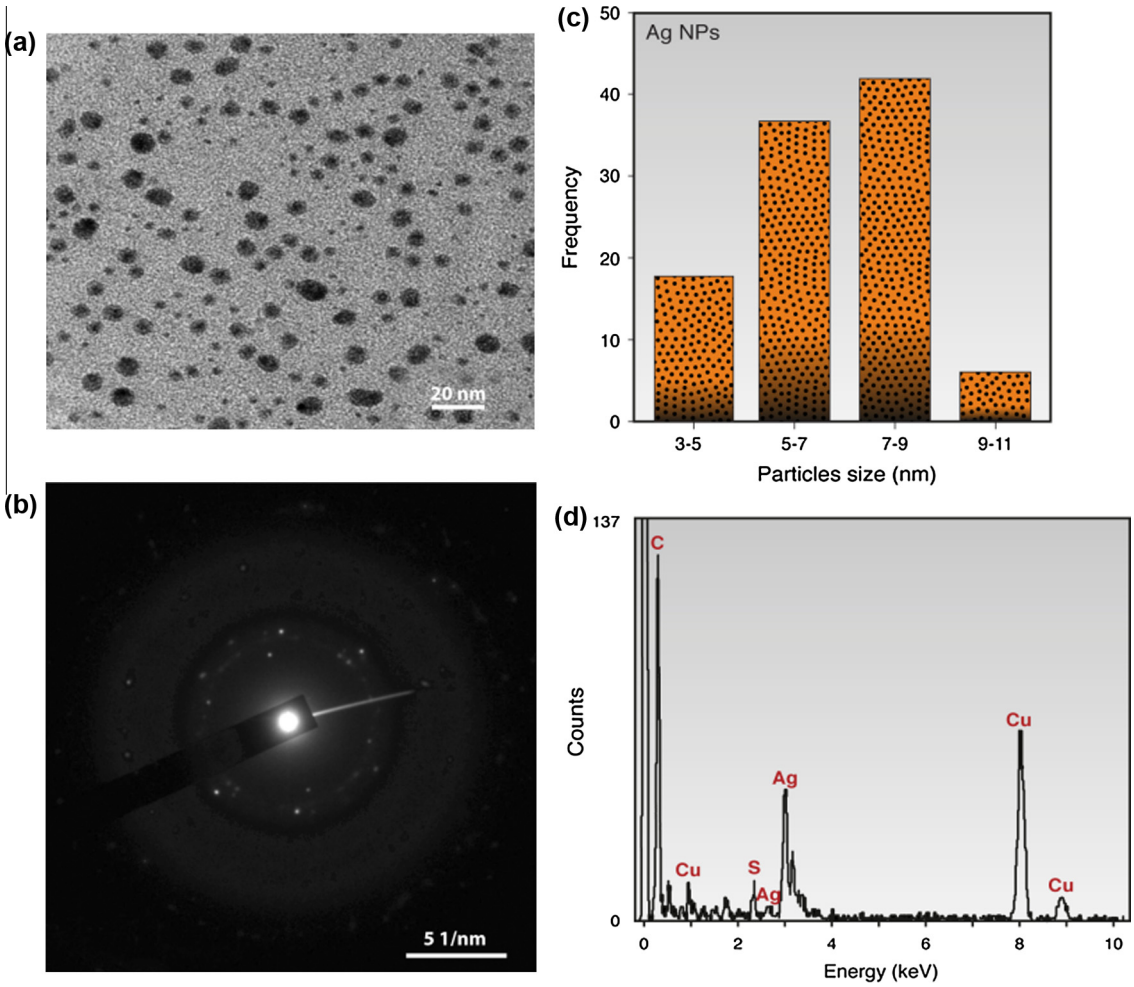

Figure 4 (a) HRTEM images of Ag NPs, (b) the selected area electron diffraction image of Ag NPs, (c) particle size distribution histogram of Ag NPs determined from HRTEM micrograph prepared at room temperature, and (d) EDS spectrum of Ag NPs from HRTEM.

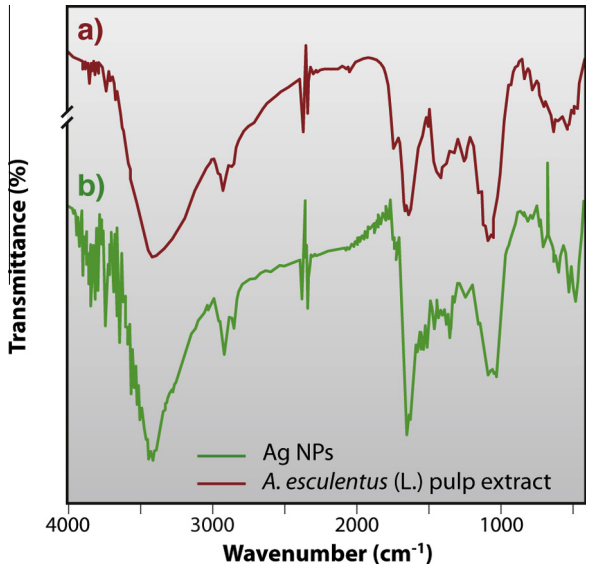

Figure 5 FTIR spectra of (a) pure *Abelmoschus esculentus* (L.) pulp extract, and (b) extract stabilized Ag NPs.

2.9.6.7. Caspase-3 activity. Involvement of apoptosis was measured by measuring caspase-3 level using ELISA according to the manufacturer's instruction (eBioscience, India). After Ag NPs exposure (0, and 16.15 μg/ml), 10 μl of Jurkat cell extracts was taken and used as samples for caspase-3 activity at 450 nm wave length.

2.9.6.8. Statistical analysis. All the parameters were repeated at least three times. The data were expressed as mean ± SEM, $n = 06$. Comparison between the mean of the control and the treated group was made by a one-way ANOVA test (using a statistical package, Origin 6.1, Northampton, MA) with multiple comparison *t*-tests, $p < 0.05$ as a limit of significance.

3. Results and discussions

3.1. UV–Vis absorption spectroscopy analysis

The optical properties of the as-synthesized Ag NPs using UV–Vis spectroscopy were studied and the recorded spectra are shown in Fig. 1. We have already mentioned that the *A. esculentus* (L.) pulp extract reduces the silver ion present in the aqueous solution resulting in the change of color of the

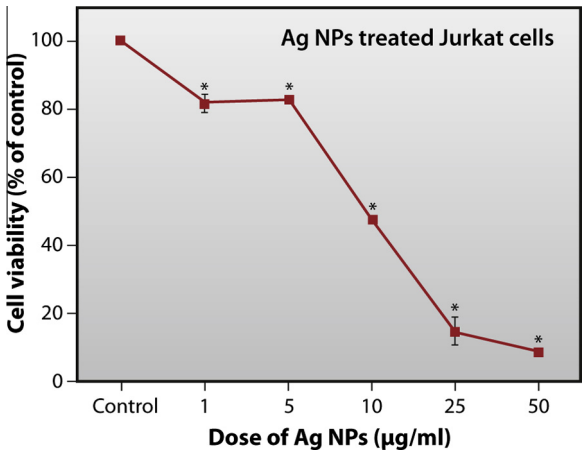

Figure 6 *In vitro* cell proliferation assay of Ag NPs treated Jurkat cell line. Values are expressed as mean ± SEM of three experiments; * indicates significant difference ($p < 0.05$) compared with the control group.

solution from colorless to light yellow due to the formation of Ag NPs. The absorption behavior shown in Fig. 1 arises due to surface plasmon resonance (SPR), which is the result of the coherent oscillation of the electrons in the conduction band of the Ag NPs induced by the electromagnetic field. It is well known that Ag NPs exhibit yellowish color in aqueous solution due to the excitation of surface plasmon vibrations in Ag NPs (Shankar et al., 2004).

Fig. 1a shows the UV–Vis spectra of the synthesized Ag NPs, which give a sharp absorbance band at around 403 nm at room temperature. To examine the stability of Ag NPs, one part of the colloidal solution of Ag NPs was left undisturbed for 8 months at room temperature and the other part was subjected to ultra-centrifugation. The obtained residue after ultra-centrifugation is homogeneously dispersed in triple distilled water by constant stirring followed by ultrasonication. UV–Vis study has been carried out with both the

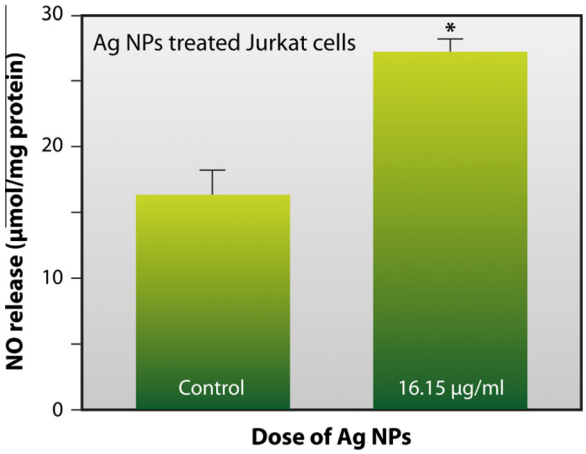

Figure 7 Nitric oxide (NO) release levels of Ag NPs treated Jurkat cell lines. The levels of NO were expressed as µmol mg^{-1} protein. Values are expressed as mean ± SEM of three experiments; * indicate significant differences ($p < 0.05$) compared with the control group.

colloidal solutions of Ag NPs, which were being restored before ultra-centrifugation and the dispersed after ultra-centrifugation (Fig. 1b). In both cases, it has been observed that there is no significant change in SPR band position or the spectral shape; only absorption intensities of Ag NPs change slightly. The above result revealed that the synthesized Ag NPs are very stable at room temperature with negligible aggregation for several months. Similar results are reported in the literature (Mollick et al., 2014a,b; Zhao et al., 2014).

3.2. X-ray diffraction (XRD) measurement

The crystalline nature of Ag NPs synthesized by reduction with *A. esculentus* (L.) pulp extract is studied by XRD analysis and given in Fig. 2. It is apparent from Fig. 2 that the characteristic peaks at 27.2°, 31.63°, 45.66°, 54.24°, and 57.04° in the 2θ region correspond to the lattice planes (220), (311), (420), (511) and (440) respectively (JCPDS No. 01-1167 and 01-1164). These results confirm the face-centered-cubic (fcc) structure of Ag NPs.

3.3. Dynamic light scattering (DLS) measurement

The dynamic light scattering (DLS) technique is used to determine the average particle size and particle size distribution profile of small particles in suspension. Fig. 3 shows the average particles size distribution of Ag NPs having a mean particle size of ~21.29 nm.

3.4. Transmission electron microscopy (TEM) measurement

TEM is employed to determine the morphology, shape and size of NPs. TEM micrographs (Fig. 4a) reveal that the particles are spherical in shape and are uniformly distributed without significant agglomeration. The selected area electron diffraction (SAED) pattern of Ag NPs prepared by *A. esculentus* (L.) pulp extract (Fig. 4b) suggests the crystalline nature of Ag NPs which is in good agreement with the X-ray diffraction (XRD) results. The NPs particle size ranges from 3 to 11 nm as seen from the particle size histogram (Fig. 4c) and possess an average size of 6.7 nm. The particle size determined by TEM is an actual diameter of the NPs as it is measured at the dried state of the sample, whereas the size measured by the dynamic light scattering method (DLS) is a hydrodynamic diameter (hydrated state). Therefore, the NPs will have a larger hydrodynamic volume due to the solvent effect in the hydrated state (Gao et al., 2008). Thus, the size of the synthesized Ag NPs observed by the TEM method is less than the size measured by the DLS method. The energy dispersive X-ray analysis (EDX) reveals a strong signal at 3 keV (Fig. 4d) which is generally shown by metallic silver nanocrystals due to surface Plasmon resonance (Magudapatty et al., 2001). There is also a strong signal for Cu in the EDX data, which originates from the carbon coated copper grid.

3.5. Fourier transform infrared (FTIR) spectroscopy analysis

The *A. esculentus* (L.) pulp extract contains different phytochemicals such as vitamins, protein, etc. which play an important role in the reduction of metal ions and the stabilization of

the nanoparticles. The *A. esculentus* (L.) pulp extract shows several characteristic bands in the FTIR spectra given in Fig. 5a. The peak at 3402 cm^{-1} is due to the N–H stretch vibrations of the peptide linkages (Kannan and John, 2008; Whiteman et al., 2008), and the peak at 2934.5 cm^{-1} corresponds to the stretching vibration of methyl groups (Li et al., 2007). The peaks at 1741.1, 1427, and 1631 cm^{-1} are attributed to carbonyl stretching vibration (Bar et al., 2009b; Luo et al., 2005), germinal methyl group (Tripathy et al., 2010), and amide I group of proteins (Whiteman et al., 2008), respectively, and the peak at 1079.7 cm^{-1} is responsible for the bending vibration of C–OH groups and the antisymmetric stretching band of C–O–C groups of polysaccharides and/or chlorophyll (Jain et al., 2011). The FTIR spectra of Ag NPs synthesized from *A. esculentus* (L.) pulp extract are given in Fig. 5b. The slight shift in peak position from 3402, 2934.5, 1741.1, 1427, 1631, and 1079.7 cm^{-1} to 3421.3, 2921.06, 1730.9, 1648, 1020.47 cm^{-1} respectively of the synthesized Ag NPs indicates that the different phytochemicals present in the *A. esculentus* (L.) pulp extract are involved in reducing and stabilizing the nanoparticles.

3.6. In vitro cell proliferation assay

Jurkat cells are exposed to Ag NPs at the concentrations of 0, 1, 10, 25 and 50 μg/ml for 24 h, and cytotoxicity is determined using a MTT assay (Fig. 6). Results have shown that Ag NPs up to the concentration of 50 μg/ ml produced a significant reduction in viability of Jurkat cells ($P > 0.05$ for each). The reduction in viability of Ag NPs treated cancer cells occurs in a dose-dependent fashion. The Ag NPs exposed Jurkat cell viability is significantly decreased by 52.6%, 85.4%, and 91.6%, at 10, 25, and 50 μg/ml doses, respectively. As shown in our previous study (Mollick et al., 2014a), the pulp extract has no anticancer components for killing the anticancer cell and it is solely caused by the Ag NPs only.

The IC_{50} value of Ag NPs against Jurkat cells is determined using the Statistica version 5.0 (Statsoft, India) software package. From this statistical calculation, it is determined that the IC_{50} value of Ag NPs is 16.15 μg/ml. As the IC_{50} value is found to be a 16.15 μg/ml concentration of Ag NPs, further experiments are carried out using this concentration to see the effect of Ag NPs against the leukemic cell line *in vitro*.

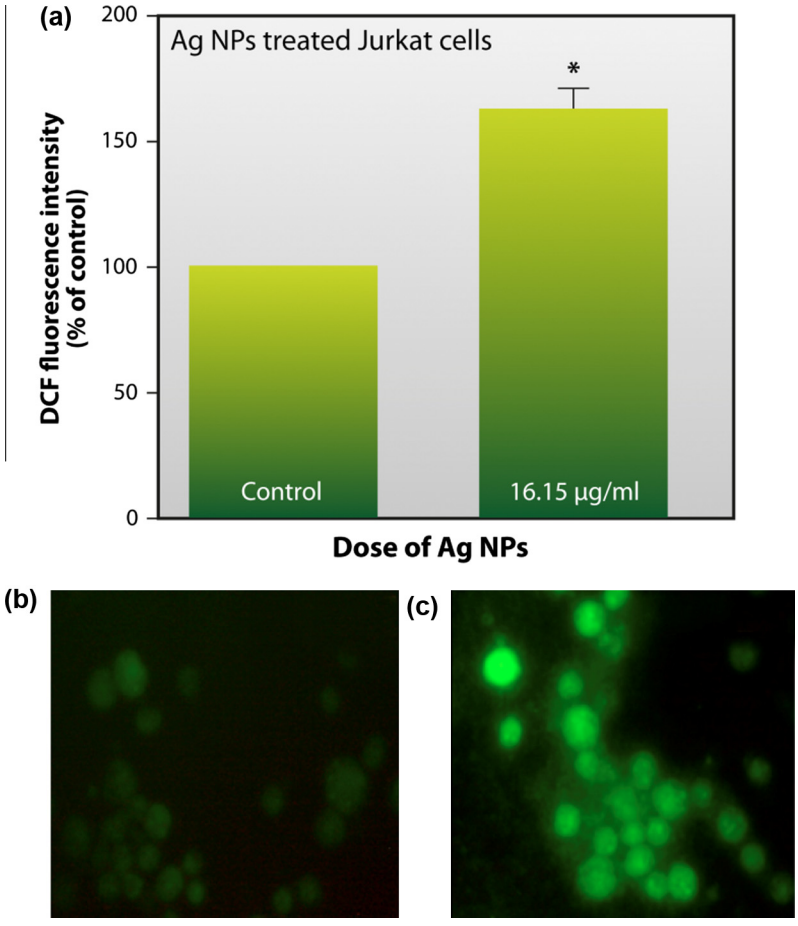

Figure 8 (a) Measurement of ROS level in Ag NPs treated Jurkat cells. DCF fluorescence intensity was expressed in term of ROS production. Values are expressed as mean ± SEM of three experiments; * indicates significant difference ($p < 0.05$) compared with the control group. Intensity of control cells was set to 100. Data are represented as the percentage of the ROS level in the control group. (b and c) Qualitative characterization of reactive oxygen species formation by $DCFH_2$-DA staining using fluorescence microscopy. Here, (b) untreated Jurkat cells, and (c) Jurkat cells treated with 16.15 μg/ml Ag NPs.

3.7. Nitric oxide (NO) release level

In the present study, Ag NPs are able to significantly ($p < 0.05$) increase the reactive nitrogen species (RNS) through NO level in Jurkat cells by 67.9% at 16.15 μg/ml dose as compared to the control (Fig. 7). It has been well established that NO reacts with superoxide to form more toxic peroxynitrite ($ONOO^-$), which has an important microbicidal and tumoricidal function. In our study, the elevated level of NO in leukemic cells may be due to severe oxidative injury, which in turn helps in cell killing ability due to Ag NPs exposure (Dash et al., 2013).

3.8. Cellular ROS level

The H_2DCFDA staining method measures intracellular generation of hydrogen peroxide, an indirect procedure for estimating ROS. In the present study, the intracellular ROS concentration is significantly ($p < 0.05$) higher in Ag NPs treated Jurkat cells when compared to the untreated control. In Jurkat cells, ROS fluorescence intensity is elevated by 60.9% at 16.15 μg/ml NPs concentration (Fig. 8a–c). ROS are chemically reactive molecules (free radicals) that play crucial functions in living organisms. In a biological system, ROS play a dual role. A moderate increase in ROS can promote cell proliferation and differentiation, whereas excessive amounts of ROS can cause oxidative damage to lipids, proteins and DNA. Therefore, maintaining cellular ROS homeostasis is crucial for normal cell growth and survival (Trachootham et al., 2009). Estimation of intracellular ROS level explores the potential role of oxidative stress as a mechanism for Ag NPs induced toxicity. Studies show that the generation or external addition of ROS can cause cell death by two distinct pathways, vis-a-vis apoptosis or necrosis (Jeyaraj et al., 2013). In our study, significant elevation of ROS due to Ag NPs exposure may be assumed as the contribution of the oxidative attack in Jurkat cell death (Foldbjerg et al., 2011).

3.9. Alterations of mitochondrial membrane potential (MMP)

Rhodamin 123 is used to measure mitochondrial membrane potential (MMP). Live cells contain mitochondria capable of retaining this dye due to higher polarity, whereas dead or apoptotic cells lose this ability because of the loss of mitochondrial membrane integrity and, thus, exhibit an extrusion of the dye (Tan et al., 2003). Because mitochondria are known to be involved in the process of programmed cell death, we investigated changes in mitochondrial membrane potential in terms

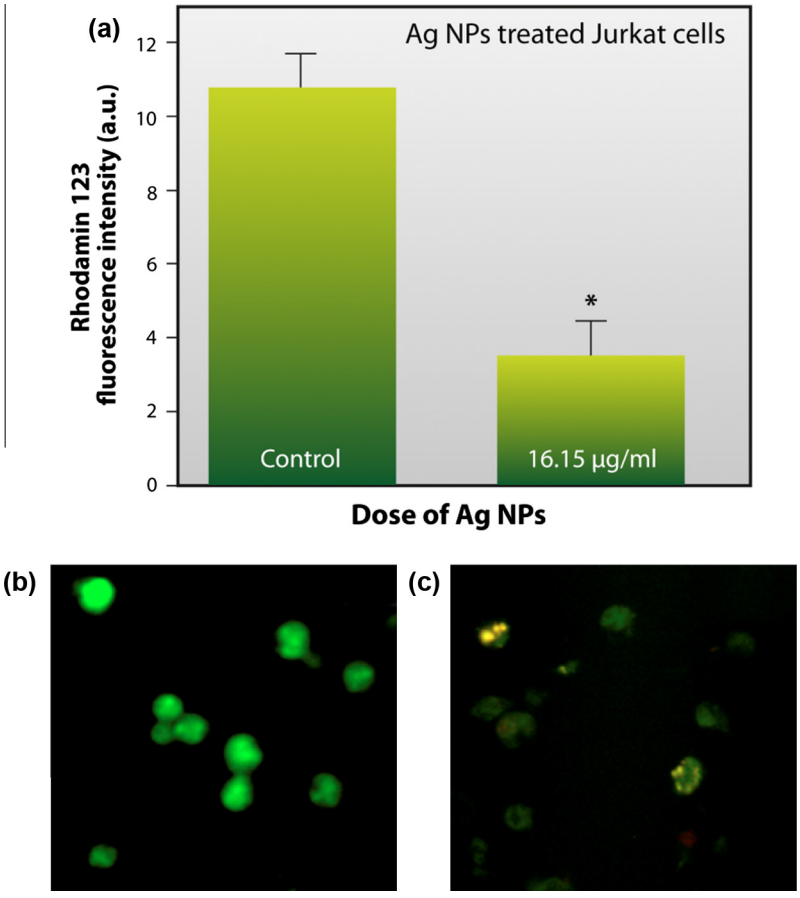

Figure 9 (a) Measurement of mitochondrial membrane potential (MMP) Ag NPs in pre-treated Jurkat cells. Values are expressed as mean ± SEM of three experiments; * indicates significant difference ($p < 0.05$) compared with the control group. (b and c) Qualitative estimation of MMP by Rh-123 staining using fluorescence microscopy. Here (b) untreated Jurkat cells, and (c) Jurkat cells treated with 16.15 μg ml Ag NPs.

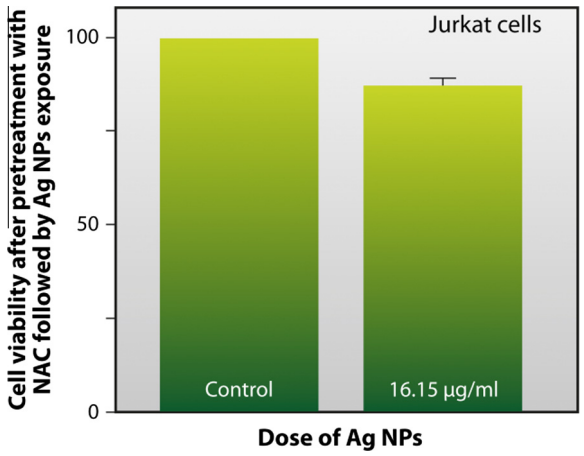

Figure 10 Quenching of ROS rescues Jurkat cells from Ag NPs induced cytotoxicity. Jurkat cells were pre-treated with 5 mM N-acetyl cysteine (NAC) for 4–6 h and then subsequently exposed to Ag NPs at IC 50 dose. Cell viability was estimated by MTT assay.

of Rh 123 fluorescence intensity. In this study, Ag NPs cause a significant depletion of MMP in Jurkat cells treated with Ag NPs for 24 h (Fig. 9a) at an IC_{50} dose. The percentage of MMP decreased significantly ($P < 0.05$) in the Jurkat cell line with the increase of Ag NPs concentration and reaches a value of 68.7% when treated with the IC_{50} dose. Depletion of MMP is also confirmed by florescence microscopic images (Fig. 9b and c). In our study, the strong dissipation in MMP in the Ag NPs exposed cancer cell line suggests a possible disruption of cellular mitochondrial membrane after Ag NPs treatment. The increased ROS levels and subsequent loss of mitochondrial membrane potential might be the reason for the involvement of apoptosis in the Ag NPs treated cells (Jeyaraj et al., 2013).

3.10. Pre-treatment with NAC

This is to confirm the main contribution of ROS in Ag NPs-induced leukemic cell death. The Jurkat cells are pre-treated with N-acetyl-L-cysteine (NAC). After these pre-treatments, NPs exposure is done at 16.15 µg/ml for 24 h, followed by experiments where cell viability is estimated using the MTT

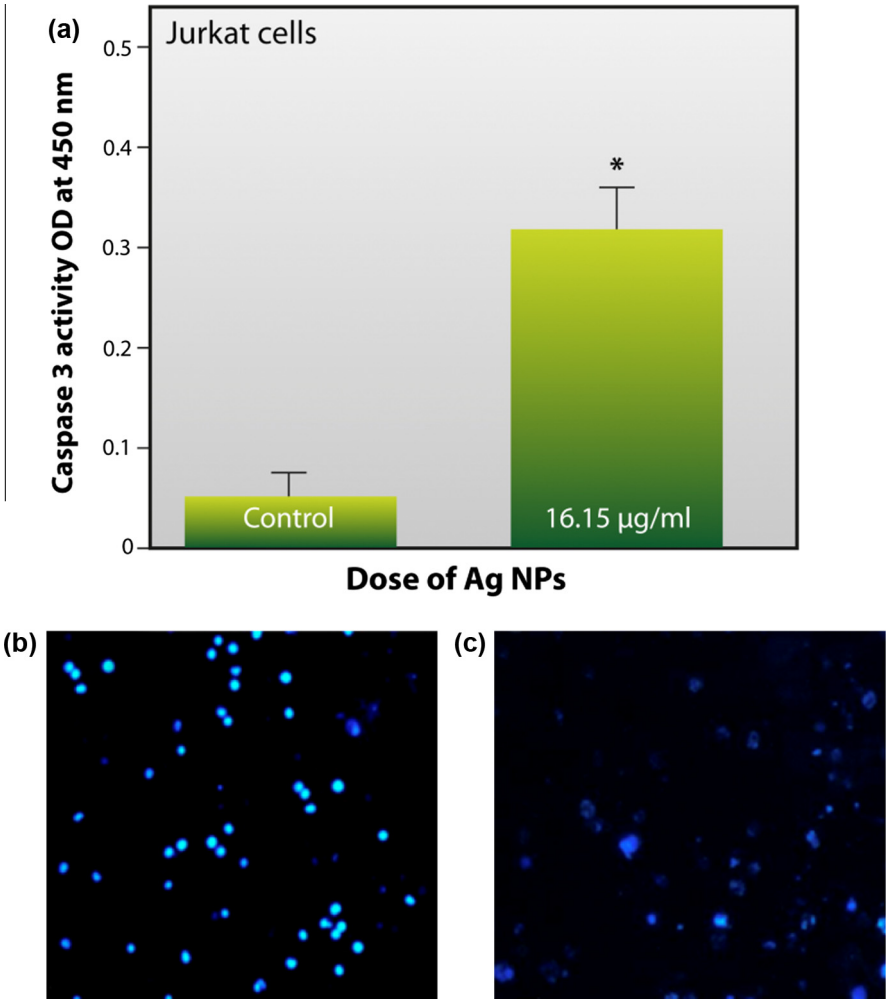

Figure 11 Increase of chromosome condensation and caspase-3 activity in Jurkat cells after exposure of Ag NPs for 24 h. (a) Caspase-3 activity; (b) control; (c) exposed to 16.15 µg/ml Ag NPs. Values are expressed as mean ± SEM of three experiments; * indicates significant difference ($p < 0.05$) compared with the control group.

method. We find that pre-treatment with NAC (ROS scavenger) protects the cells from the cytotoxic effects of NPs. In these cases, >85% of cell viability suggests that Ag NPs selectively kill the leukemic cells by generation of ROS (Fig. 10).

3.11. Induction of caspase-3 activity and chromosome condensation by Ag NPs

The disruption of cellular metabolic activity of Jurkat cells followed by Ag NPs exposure seems to be affected by apoptosis phenomenon. Thus, involvement of apoptosis was investigated by caspase-3 assay. Caspase-3, considered to be the most significant of the executioner caspases resulting in cellular apoptosis, was induced following exposure with Ag NPs (Fig. 11a). When Jurkat cells were treated with IC_{50} concentrations of Ag NPs for 24 h, caspase-3 activity was significantly ($p < 0.05$) increased with compare to untreated cells. Chromatin condensation was also noted by DAPI staining with the addition to the caspase-3 activity. When Jurkat cells were treated with the IC_{50} concentrations of Ag NPs for 24 h, chromatin condensation and fragmentation were observed in the treated group (Fig. 11b and c). Caspase-3 activation and chromatin condensation/fragmentation in Jurkat cells suggest that Ag NPs caused cell death was mainly due to apoptotic process (Gurunathan et al., 2013; Mollick et al., 2014a).

3.12. Antimicrobial activity of silver nanoparticles against microorganisms

The Ag NPs solution exhibits excellent antibacterial activity against the bacteria, *B. subtilis*, *B. cereus*, *E. coli*, *M. luteus* and *P. aeruginosa*, by showing the clearing zone around the holes with bacterial growth on petri plates by the cup plate method. The radial diameter of the inhibiting zones of *B. subtilis*, *B. cereus*, *E. coli*, *M. luteus*, and *P. aeruginosa* is 33, 28, 19, 40, and 26 mm, respectively. The Ag NPs at the concentration of 0.2 mg/ml show a range of specificity toward their antimicrobial activity (Fig. 12). Fig. 13 represents the clear inhibition zone made by the Ag NPs solution against only

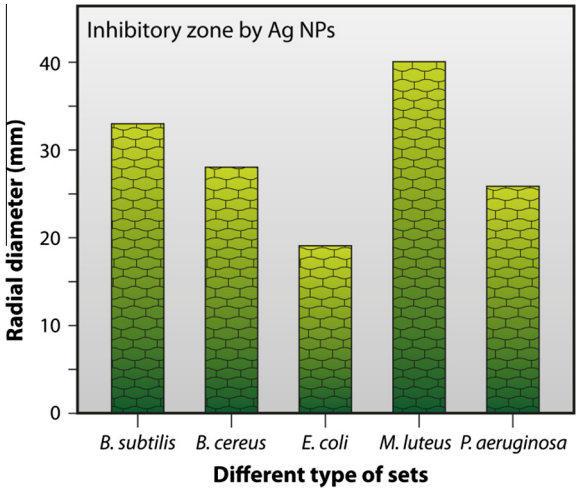

Figure 12 Histogram shows the radial diameter of inhibitory zone by Ag NPs at the same concentration (0.2 mg/ml) against different microorganisms.

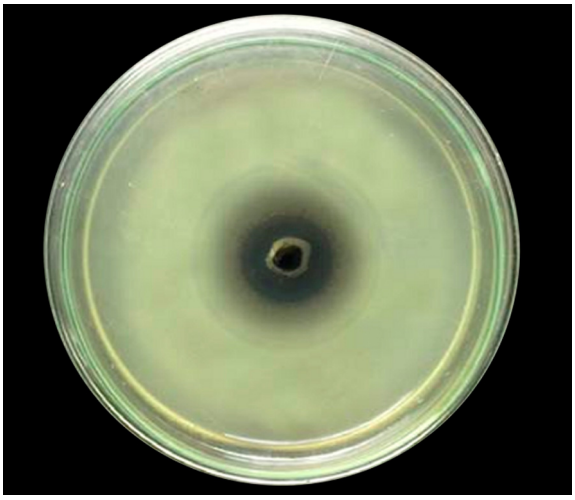

Figure 13 Antibacterial activity of Ag NPs assayed by the agar diffusion method in petri plate. Ag NPs, poured in the circular well, showed the zone of inhibition against *Bacillus subtilis*. The cavity of the petri plate was filled with Ag NPs solution (0.2 mg/ml).

the strain of *B. subtilis*. The clear zone indicates bacterial growth restriction by the diffused Ag NPs solution. At the same time, the control sets did not show any inhibition. Results are the mean of three separate experiments, each in triplicate. Thus, the synthesized Ag NPs have great potential due to their antibacterial activity.

4. Conclusions

We demonstrate an eco-friendly and low cost synthesis procedure of small size Ag NPs using *A. esculentus* (L.) pulp solution. Crystalline Ag NPs of average diameter ~6.7 nm are successfully employed in both antibacterial and anticancer activity. Based on these findings, Ag NPs may lead to valuable applications in various fields such as medicinal and as antimicrobial agents. The synthesized Ag NPs are capable of showing anti-proliferative effects in a dose dependent manner with an IC_{50} value of 16.15 μg/ml. It is also observed that anticancer activity of Ag NPs is strongly associated with an increased level of reactive oxygen species (ROS) and reactive nitrogen species with the loss of mitochondrial membrane integrity. Pre-treatment with N-acetyl-L-cysteine suggests that Ag NPs mediated Jurkat cell killing is mainly due to excess production of the ROS level. Thus, we have effectively synthesized Ag NPs using the green route and have demonstrated their potential therapeutic uses.

Acknowledgements

The authors Md. M.R. Mollick and S. Pattanayak gratefully acknowledge the Department of Science & Technology (DST), Govt. of India for providing fellowship under the INSPIRE program. B. Bhowmick wishes to thank the Council of Scientific & Industrial Research (CSIR) Project [02 (0077)/12/EMR-II dated 01.11.2012] and D. Mondal likes to thank the CSIR, New Delhi for his fellowship. We also

acknowledge the Center for Research in Nanoscience and Nanotechnology (CRNN), University of Calcutta and USIC (Vidyasagar University) for instrumental facilities.

References

AshaRani, P.V., Low Kah Mun, G., Hande, M.P., Valiyaveettil, S., 2009. Cytotoxicity and enotoxicity of silver nanoparticles in human cells. ACS Nano 3, 279–290.

Bankura, K.P., Maity, D., Mollick, M.M.R., Mondal, D., Bhowmick, B., Bain, M.K., Chakraborty, A., Sarkar, J., Acharya, K., Chattopadhyay, D., 2012. Synthesis, characterization and antimicrobial activity of dextran stabilized silver nanoparticles in aqueous medium. Carbohydr. Polym. 89, 1159–1165.

Bar, H., Bhui, D.K., Sahoo, G.P., Sarkar, P., De, S.P., Misra, A., 2009a. Green synthesis of silver nanoparticles using latex of *Jatropha curcas*. Colloids Surf., A 339, 134–139.

Bar, H., Bhui, D.K., Sahoo, G.P., Sarkar, P., Pyne, S., Misra, A., 2009b. Green synthesis of silver nanoparticles using seed extract of *Jatropha curcas*. Colloids Surf., A 348, 212–216.

Bhushan, B., 2004. Springer Handbook of Nanotechnology. Springer-Verlag, Heidelberg.

Callegari, A., Tonti, D., Chergui, M., 2003. Photochemically grown silver nanoparticles with wavelength-controlled size and shape. Nano Lett. 3, 1565–1568.

Canadian Cancer Society/National Cancer Institute of Canada, 2005. Canadian Cancer Statistics.

Dash, S.K., Chattopadhyay, S., Ghosh, T., Tripathy, S., Das, S., Das, D., Roy, S., 2013. Antileukemic efficacy of monomeric manganese-based metal complex on KG-1A and K562 cell lines. ISRN Oncol. 2013, 709269 (pp. 10).

Devi, J.S., Bhimba, B.V., Ratnam, K., 2012. In vitro anticancer activity of silver nanoparticles synthesized using the extract of *Gelidiella sp*. Int. J. Pharm. Pharm. Sci. 4, 710–715.

Dimitrijevic, N.M., Bartels, D.M., Jonah, C.D., Takahashi, K., Rajh, T., 2001. Radiolytically induced formation and optical absorption spectra of colloidal silver nanoparticles in supercritical ethane. J. Phys. Chem. B 105, 954–959.

Foldbjerg, R., Dang, D.A., Autrup, H., 2011. Cytotoxicity and genotoxicity of silver nanoparticles in the human lung cancer cell line, A549. Arch. Toxicol. 85, 743–750.

Gao, F.P., Zhang, H.Z., Liu, L.R., Wang, Y.S., Jiang, Q., Yang, X.D., Zhang, Q.Q., 2008. Preparation and physicochemical characteristics of self-assembled nanoparticles of deoxycholic acid modified-carboxymethyl curdlan conjugates. Carbohydr. Polym. 71, 606–613.

Gardea-Torresdey, J.L., Parsons, J.G., Gomez, E., Peralta-Videa, J., Troiani, H.E., Santiago, P., Yacaman, M. Jose, 2002. Formation and growth of Au nanoparticles inside live Alfalfa plants. Nano Lett. 2, 397–401.

Gardea-Torresdey, J.L., Gomez, E., Peralta-Videa, J.R., Parsons, J.G., Troiani, H., Jose, Yacaman.M., 2003. Alfalfa sprouts: a natural source for the synthesis of silver nanoparticles. Langmuir 19, 1357–1361.

Garrett, M., Workman, P., 1999. Discovering novel chemotherapeutic drugs for the third millennium. Eur. J. Cancer 35, 2010–2030.

Gurunathan, S., Han, J.W., Eppakayala, V., Jeyaraj, M., Kim, J.H., 2013. Cytotoxicity of biologically synthesized silver nanoparticles in MDA-MB-231 human breast cancer cells. Biomed. Res. Int. 2013, 535796 (pp. 10).

Hanley, C., Thurber, A., Hanna, C., Punnoose, A., Zhang, J., Wingett, D.G., 2009. The influences of cell type and ZnO nanoparticle size on immune cell cytotoxicity and cytokine induction. Nanoscale Res. Lett. 4, 1409–1420.

Hernandez-Sierra, J.F., Ruiz, F., Pena, D.C.C., Martinez-Gutierrez, F., Martinez, A.E., Guillen, A.J.P., Tapia-Perez, H., Castanon, G.M., 2008. The antimicrobial sensitivity of *Streptococcus mutans* to nanoparticles of silver, zinc oxide, and gold. Nanomed. Nanotechnol. Biol. Med. 4, 237–240.

Jain, N., Bhargava, A., Majumdar, S., Tarafdar, J.C., Panwar, J., 2011. Extracellular biosynthesis and characterization of silver nanoparticles using *Aspergillus flavus* NJP08: a mechanism perspective. Nanoscale 3, 635–641.

Jeyaraj, M., Rajesh, M., Arun, R., MubarakAli, D., Sathishkumar, G., Sivanandhan, G., Dev, G.K., Manickavasagam, M., Premkumar, K., Thajuddin, N., Ganapathi, A., 2013. An investigation on the cytotoxicity and caspase-mediated apoptotic effect of biologically synthesized silver nanoparticles using *Podophyllum hexandrum* on human cervical carcinoma cells. Colloids Surf., B 102, 708–717.

Kannan, P., John, S.A., 2008. Synthesis of mercaptothiadiazole-functionalized gold nanoparticles and their self-assembly on Au substrates. Nanotechnology 19, 085602 (pp. 10).

Klaus, T., Joerger, R., Olsson, E., Granqvist, C.G., 1999. Silver-based crystalline nanoparticles, microbially fabricated. Proc. Natl. Acad. Sci. USA 96, 13611–13614.

Konishi, Y., Ohno, K., Saitoh, N., Nomura, T., Nagamine, S., Hishida, H., Takahashi, Y., Uruga, T., 2007. Bioreductive deposition of platinum nanoparticles on the bacterium *Shewanella algae*. J. Biotechnol. 128, 648–653.

Kora, A.J., Sashidhar, R.B., Arunachalam, J., 2010. Gum kondagogu (*Cochlospermum gossypium*): a template for the green synthesis and stabilization of silver nanoparticles with antibacterial application. Carbohydr. Polym. 82, 670–679.

Krutyakov, Y.A., Kudrynskiy, A.A., Olenin, A.Y., Lisichkin, G.V., 2008. Synthesis and properties of silver nanoparticles: advances and prospects. Russ. Chem. Rev. 77, 233–257.

Kumar, R., Roopan, S.M., Prabhakarn, A., Khanna, V.G., Chakroborty, S., 2012. Agricultural waste *Annona squamosa* peel extract: biosynthesis of silver nanoparticles. Spectrochim. Acta A 90, 173–176.

Kumar, D.A., Palanichamy, V., Roopan, S.M., 2014. Green synthesis of silver nanoparticles using *Alternanthera dentata* leaf extract at room temperature and their antimicrobial activity. Spectrochim. Acta A 127, 168–171.

Li, S., Shen, Y., Xie, A., Yu, X., Qiu, L., Zhang, L., Zhang, Q., 2007. Green synthesis of silver nanoparticles using *Capsicum annuum L.* extract. Green Chem. 9, 852–858.

Luo, L.B., Yu, S.H., Qian, H.S., Zhou, T., 2005. Large-scale fabrication of flexible silver/cross-linked poly(vinyl alcohol) coaxial nanocables by a facile solution approach. J. Am. Chem. Soc. 127, 2822–2823.

Madhumitha, G., Elango, G., Roopan, S.M., 2015. Bio-functionalized doped silver nanoparticles and its antimicrobial studies. J. Sol-Gel. Sci. Technol. 73, 476–483.

Magudapatty, P., Gangopadhyayrans, P., Panigrahi, B.K., Nair, K.G.M., Dhara, S., 2001. Electrical transport studies of Ag nanoparticles embedded in glass matrix. Physica B 299, 142–146.

Mahapatra, S. Kar, Chakraborty, S.P., Das, S., Roy, S., 2009. Methanol extract of Ocimum gratissimum protects murine peritoneal macrophages from nicotine toxicity by decreasing free radical generation, lipid and protein damage and enhances antioxidant protection. Oxid. Med. Cell Longev. 2, 222–230.

Maity, D., Bain, M.K., Bhowmick, B., Sarkar, J., Saha, S., Acharya, K., Chakraborty, M., Chattopadhyay, D., 2011. In situ synthesis, characterization, and antimicrobial activity of silver nanoparticles using water soluble polymer. J. Appl. Polym. Sci. 122, 2189–2196.

Maity, D., Mollick, M.M.R., Mondal, D., Bhowmick, B., Bain, M.K., Bankura, K., Sarkar, J., Acharya, K., Chattopadhyay, D., 2012. Synthesis of methylcellulose–silver nanocomposite and investigation of mechanical and antimicrobial properties. Carbohydr. Polym. 90, 1818–1825.

Mishra, A., Tripathy, S.K., Yun, S., 2011. Bio-synthesis of gold and silver nanoparticles from *Candida guilliermondii* and their antimicrobial effect against pathogenic bacteria. J. Nanosci. Nanotechnol. 11, 243–248.

Mohan, Y.M., Raju, K.M., Sambasivudu, K., Singh, S., Sreedhar, B., 2007. Preparation of acacia-stabilized silver nanoparticles: a green approach. J. Appl. Polym. Sci. 106, 3375–3381.

Mollick, M.M.R., Bhowmick, B., Maity, D., Mondal, D., Bain, M.K., Bankura, K., Sarkar, J., Rana, D., Acharya, K., Chattopadhyay, D., 2012. Green synthesis of silver nanoparticles using *Paederia foetida L.* leaf extract and assessment of their antimicrobial activities. Int. J. Green Nanotechnol. 4, 230–239.

Mollick, M.M.R., Bhowmick, B., Mondal, D., Maity, D., Rana, D., Dash, S.K., Chattopadhyay, S., Roy, S., Sarkar, J., Acharya, K., Chakraborty, M., Chattopadhyay, D., 2014a. Anticancer (*in vitro*) and antimicrobial effect of gold nanoparticles synthesized using *Abelmoschus esculentus* (L.) pulp extract *via* a green route. RSC Adv. 4, 37838–37848.

Mollick, M.M.R., Bhowmick, B., Maity, D., Mondal, D., Roy, I., Sarkar, J., Rana, D., Acharya, K., Chattopadhyay, S., Chattopadhyay, D., 2014b. Green synthesis of silver nanoparticle based nanofluids and investigation of their antimicrobial activities. Microfluid. Nanofluid. 16, 541–551.

Mukherjee, P., Ahmad, A., Mandal, D., Senapati, S., Sainkar, S.R., Khan, M.I., Ramani, R., Parischa, R., Ajaykumar, P.V., Alam, M., Sastry, M., Kumar, R., 2001a. Bioreduction of $AuCl_4^-$ ions by the fungus, Verticillium sp. and surface trapping of the gold nanoparticles formed. Angew. Chem. Int. Ed. 40, 3585–3588.

Mukherjee, P., Ahmad, A., Mandal, D., Senapati, S., Sainkar, S.R., Khan, M.I., Ramani, R., Parischa, R., Ajaykumar, P.V., Alam, M., Kumar, R., Sastry, M., 2001b. Fungus mediated synthesis of silver nanoparticles and their immobilization in the mycelial matrix: a novel biological approach to nanoparticle synthesis. Nano Lett. 1, 515–519.

Naik, R.R., Stringer, S.J., Agarwal, G., Jones, S., Stone, M.O., 2002. Biomimetic synthesis and patterning of silver nanoparticles. Nat. Mater. 1, 169–172.

Perrin, D.D., Armarigo, W.L.F., Perrin, D.R., 1980. Purification of Laboratory Chemicals, second ed. Pergamon Press, Oxford, UK.

Roopan, S.M., Elango, G., 2015. Exploitation of *Cocos nucifera* a non-food toward the biological and nanobiotechnology field. Ind. Crop. Prod. 67, 130–136.

Roopan, S.M., Rohit, Madhumitha, G., Rahuman, A.A., Kamaraj, C., Bharathi, A., Surendra, T.V., 2013. Low-cost and eco-friendly phyto-synthesis of silver nanoparticles using *Cocos nucifera* coir extract and its larvicidal activity. Ind. Crop. Prod. 43, 631–635.

Roopan, S.M., Kumar, S.H.S., Madhumitha, G., Suthindhiran, K., 2015. Biogenic-production of SnO_2 nanoparticles and its cytotoxic effect against hepatocellular carcinoma cell line (HepG2). Appl. Biochem. Biotechnol. 175, 1567–1575.

Rosenberg, B., VanCamp, L., Trosko, J.E., Mansour, V.H., 1969. Platinum compounds: a new class of potent antitumour agents. Nature 222, 385–386.

Roy, A., Ganguly, A., BoseDasgupta, S., Das, B.B., Pal, C., Jaisankar, P., Majumder, H.K., 2008. Mitochondria-dependent reactive oxygen species-mediated programmed cell death induced by 3,3-diindolylmethane through inhibition of F0F1-ATP synthase in unicellular protozoan parasite Leishmania donovani. Mol. Pharmacol. 74, 1292–1307.

Saha, S., Sarkar, J., Chattopadhyay, D., Patra, S., Chakraborty, A., Acharya, K., 2010. Production of silver nanoparticles by a phytopathogenic fungus bipolaris nodulosa and its antimicrobial activity. Dig. J. Nanomater. Biostruct. 5, 887–895.

Sanpui, P., Chattopadhyay, A., Ghosh, S.S., 2011. Induction of apoptosis in cancer cells at low silver nanoparticle concentrations using chitosan nanocarrier. ACS Appl. Mater. Interfaces 3, 218–228.

Sarkar, J., Saha, S., Chattopadhyay, D., Patra, S., Acharya, K., 2011. Mycosynthesis of silver nanoparticles and investigation of their antimicrobial activity. J. Nanosci. Nanoeng. Appl. 1, 17–26.

Satyavani, K., Ramanathan, T., Gurudeeban, S., 2011. Green synthesis of silver nanoparticles by using stem derived callus extract of Bitter apple (Citrullus colocynthis). Dig. J. Nanomater. Biostruct. 6, 1019–1024.

Shankar, S., Ahmad, A., Sastry, M., 2003. Geranium leaf assisted biosynthesis of silver nanoparticles. Biotechnol. Prog. 19, 1627–1631.

Shankar, S.S., Rai, A., Ahmad, A., Sastry, M., 2004. Rapid synthesis of Au, Ag, and bimetallic Au core–Ag shell nanoparticles using Neem (*Azadirachta indica*) leaf broth. J. Colloid Interface Sci. 275, 496–502.

Sharma, V.K., Yngard, R.A., Lin, Y., 2009. Silver nanoparticles: green synthesis and their antimicrobial activities. Adv. Colloid Interface Sci. 145, 83–96.

Silver, S., 2003. Bacterial silver resistance. molecular biology and uses and misuses of silver compounds. FEMS Microbiol. Rev. 27, 341–353.

Song, J.Y., Kim, B.S., 2009. Rapid biological synthesis of silver nanoparticles using plant leaf extracts. Bioprocess Biosyst. Eng. 32, 79–84.

Sun, Y., Yin, Y., Mayers, B.T., Herricks, T., Xia, Y., 2002. Uniform silver nanowires synthesis by reducing $AgNO_3$ with ethylene glycol in the presence of seeds and poly(vinyl pyrrolidone). Chem. Mater. 14, 4736–4745.

Swami, A., Selvakannan, P.R., Pasricha, R., Sastry, M., 2004. One-step synthesis of ordered two-dimensional assemblies of silver nanoparticles by the spontaneous reduction of silver ions by pentadecylphenol Langmuir monolayers. J. Phys. Chem. B 108, 19269–19275.

Tan, Y., Yu, R., Pezzuto, J.M., 2003. Betulinic acid-induced programmed cell death in human melanoma cells involves mitogen-activated protein kinase activation. Clin. Cancer Res. 9, 2866–2875.

Trachootham, D., Alexandre, J., Huang, P., 2009. Targeting cancer cells by ROS-mediated mechanisms: A radical therapeutic approach? Nat. Rev. Drug Discov. 8, 579–591.

Tripathy, A., Raichur, A.M., Chandrasekaran, N., Prathna, T.C., Mukherjee, J., 2010. Process variables in biomimetic synthesis of silver nanoparticles by aqueous extract of *Azadirachta indica* (Neem) leaves. J. Nanopart. Res. 12, 237–246.

Whiteman, S.C., Yang, Y., Jones, J.M., Spiteri, M.A., 2008. FTIR spectroscopic analysis of sputum: preliminary findings on a potential novel diagnostic marker for COPD. Ther. Adv. Respir. Dis. 2, 23–31.

Willner, I., Baron, R., Willner, B., 2006. Growing metal nanoparticles by enzymes. Adv. Mater. 18, 1109–1120.

Yin, B., Ma, H., Wang, S., Chen, S., 2003. Electrochemical synthesis of silver nanoparticles under protection of poly(*N*-vinylpyrrolidone). J. Phys. Chem. B 107, 8898–8904.

Zhang, L., Shen, Y.H., Xie, A.J., Li, S.K., Jin, B.K., Zhang, Q.F., 2006. One-step synthesis of monodisperse silver nanoparticles beneath vitamin E Langmuir monolayers. J. Phys. Chem. B 110, 6615–6620.

Zhao, X., Xia, Y., Li, Q., Ma, X., Quan, F., Geng, C., Han, Z., 2014. Microwave-assisted synthesis of silver nanoparticles using sodium alginate and their antibacterial activity. Colloids Surf., A 444, 180–188.

Please cite this article in press as: Mollick, M.M.R. et al., Studies on green synthesized silver nanoparticles using *Abelmoschus esculentus* (L.) pulp extract having anticancer (*in vitro*) and antimicrobial applications. Arabian Journal of Chemistry (2015), http://dx.doi.org/10.1016/j.arabjc.2015.04.033